Nagao et al., http://www.jcb.org/cgi/content/full/jcb.200807130/DC1

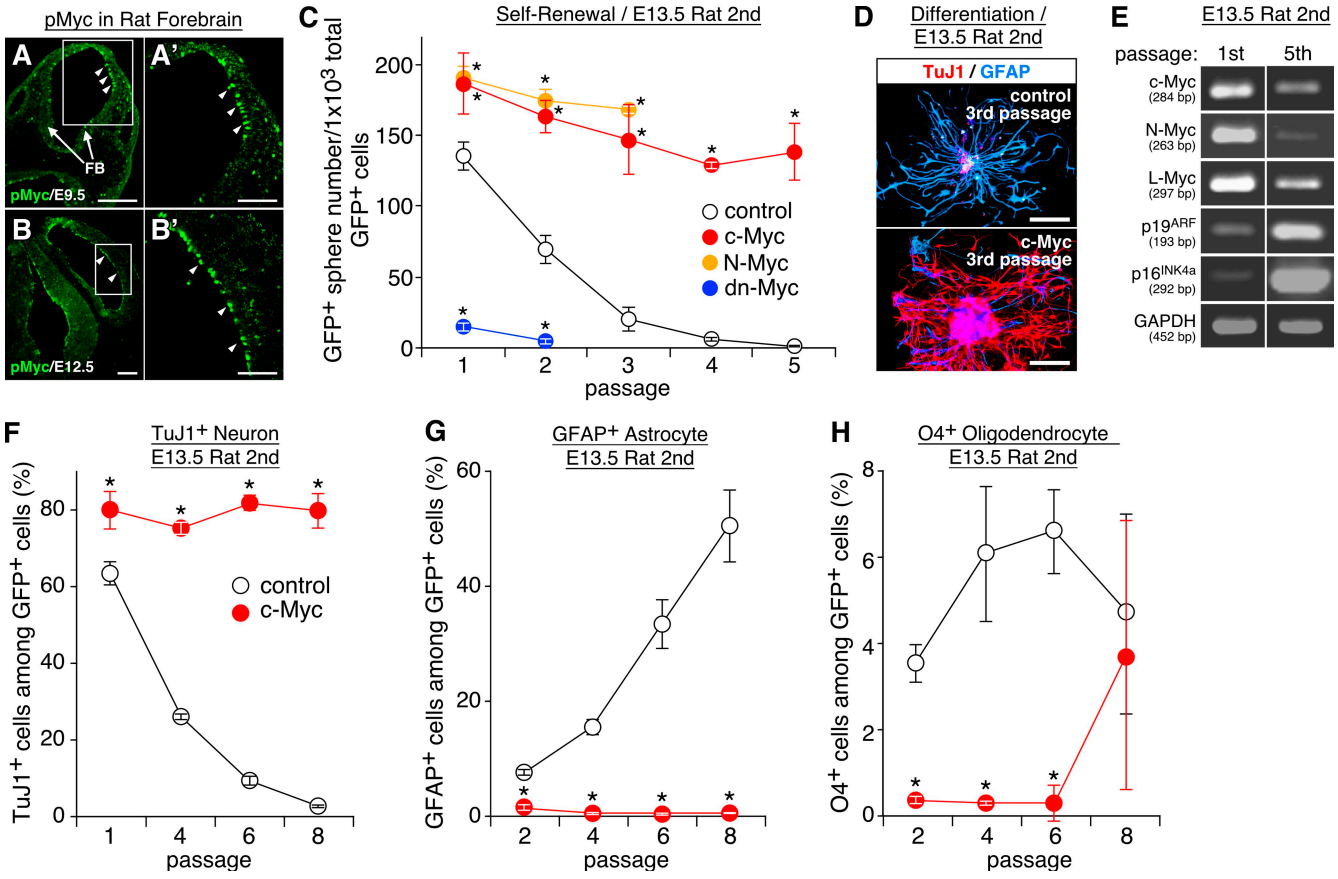

Figure S1. **Myc-dependent regulation of self-renewal and differentiation during serial passages of neurospheres.** (A–B′) The expression of Myc (pMyc) in proliferating cells on the apical side of the forebrain (FB) neuroepithelium at E9.5 (A) and 12.5 (B). A′ and B′ are higher magnification views of the boxed areas in A and B, respectively. Immunostaining using an antibody for phosphorylated forms of c-Myc and N-Myc (pMyc), which are selectively expressed at the M phase of the cell cycle (Luscher, B., and R.N. Eisenman. 1992. *J. Cell Biol.* 118:775–784), detected nuclei on the apical side of the developing neural tube (arrowheads), indicating that Myc is expressed in proliferating cells. (C–H) Changes in the properties of neurospheres during serial passages in vitro. Secondary neurospheres derived from E13.5 rat embryonic forebrains were infected with retroviruses expressing c-Myc, N-Myc, and dn-Myc and were subsequently passaged serially at a clonal density in methylcellulose matrix (see Materials and methods). The self-renewal (C) and differentiation (D and F–H) potential was compared among cells obtained by different passages (first eighth). D shows photographs of control (top) and c-Myc (bottom) virus–infected clonal spheres that were passaged three times, induced to differentiate, and subsequently double stained for TuJ1 (red) and GFAP (blue). E shows the comparison of the expression levels of c-Myc, N-Myc, L-Myc, $p19^{ARF}$, and $p16^{INK4a}$ between the first and fifth passage neurospheres. The sizes of PCR products are shown in base pairs below the gene names. *, $P < 0.01$ compared with control virus–infected cells. Error bars indicate mean + SD. Bars: (A and B) 200 µm; (A′, B′, and D) 100 µm.

A Rat tissue (Figure 1D)

	Normalized relative mRNA expression				
	E13.5	E16.5	E18.5	P2	Adult SVZ
c-Myc	1.00 ± 0.37	0.82 ± 0.07	1.09 ± 0.18	1.29 ± 0.14	0.08 ± 0.01
$p19^{ARF}$	1.00 ± 0.10	2.75 ± 0.19*	3.37 ± 0.20*	18.94 ± 2.19*	12.55 ± 1.01*

B Rat neurosphere (Figure 1E and 1G)

	E13.5	E18.5	Adult SVZ
c-Myc	1.00 ± 0.18	1.04 ± 0.30	1.01 ± 0.13
$p19^{ARF}$	1.00 ± 0.16	4.00 ± 0.49*	20.09 ± 4.91*

C Mouse neurosphere & MEF (Figure 1F)

	E11.5	E18.5	MEF WT	MEF *p53*$^{-/-}$
$p19^{ARF}$	1.00 ± 0.50	8.42 ± 1.21*	3.18 ± 0.33*	16.00 ± 1.83*

D Rat neurosphere (Figure 5A)

	E13.5 1st	E13.5 5th
c-Myc	1.00 ± 0.18	0.49 ± 0.05*
$p19^{ARF}$	1.00 ± 0.16	19.49 ± 3.22*

E E13.5 rat neurosphere 8th passage (Figure 5B)

	control	c-Myc
$p19^{ARF}$	1.00 ± 0.36	0.12 ± 0.02*

F E13.5 rat neurosphere (Figure 5C)

	FGF2/EGF	FGF2/EGF+CNTF
N-Myc	1.00 ± 0.37	0.04 ± 0.01*
$p19^{ARF}$	1.00 ± 0.14	5.35 ± 0.22*

Figure S2. **Developmental and extracellular signal-dependent changes in the expression level of Myc and $p19^{ARF}$.** (A–F) The expression level of mRNAs for Myc and $p19^{ARF}$ in various samples was quantified by RT-PCR using Opticon DNA Engine (Bio-Rad Laboratories). GAPDH was used as an internal control. Figures showing corresponding images of amplified products run in agarose gels are indicated in each panel. *, $P < 0.01$ compared with the values shown in the leftmost column (designated as 1.0). Data are expressed as mean + SD. SVZ, subventricular zone; MEF, mouse embryo fibroblast.

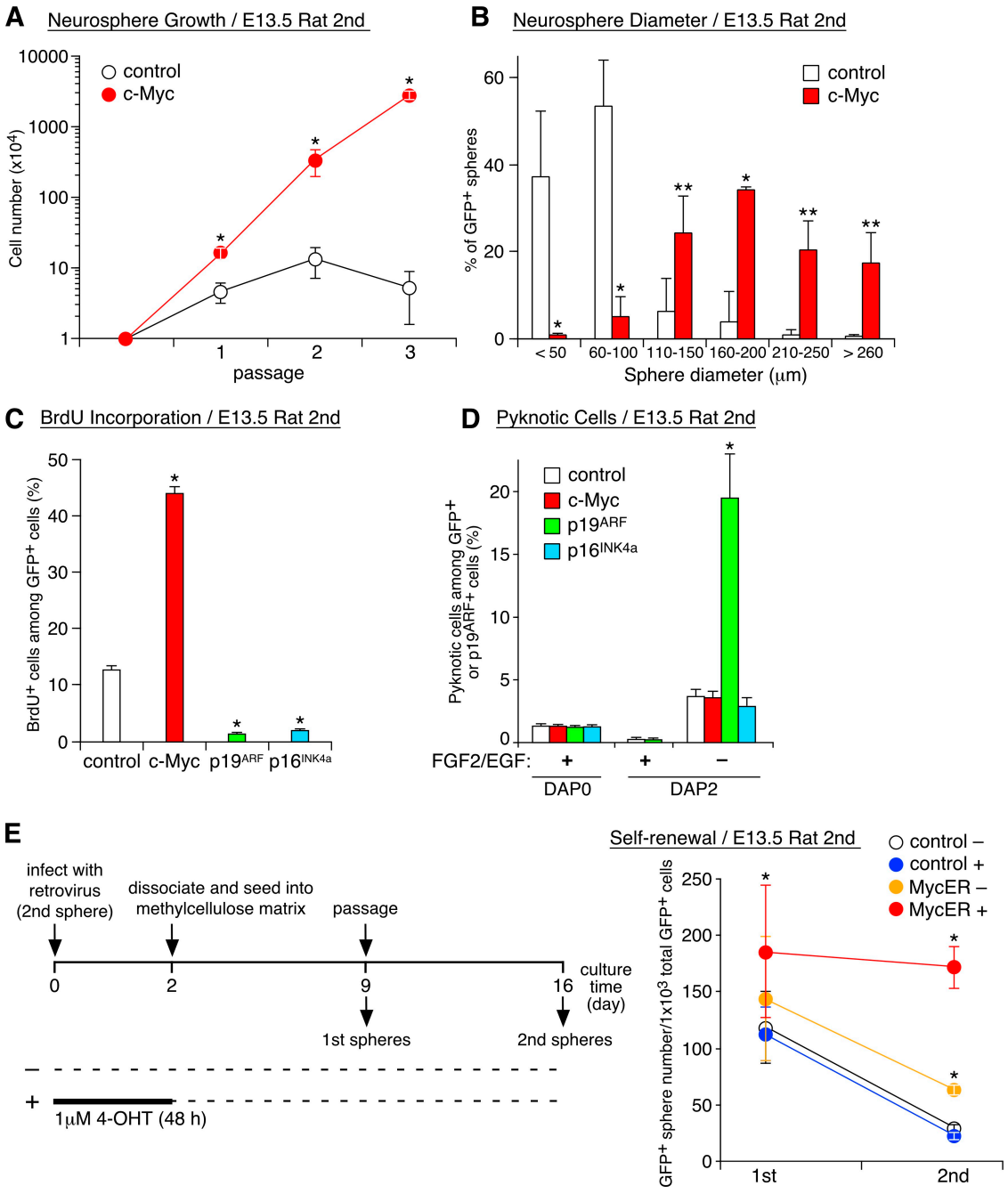

Figure S3. **Modulation of cell growth and death by c-Myc and p19^{ARF}.** (A and B) Stimulation of NSC growth by c-Myc. E13.5 embryo-derived secondary neurospheres were infected with control and c-Myc viruses and grown at a clonal density. Cells were passaged once every week, and the number of total viable cells (A) and diameter of individual spheres after the first passage (B) were examined. (C) Antagonistic action of c-Myc and p19^{ARF} on NSC growth. Neurospheres infected with control, c-Myc, p19^{ARF}, and p16^{INK4a} viruses were labeled with BrdU for 2 h in the presence of FGF2 and EGF, and the percentage of BrdU$^+$ cells among total infected cells was quantified. (D) Effects of c-Myc, p19^{ARF}, and p16^{INK4a} on cell death. Neurospheres infected with control, c-Myc, p19^{ARF}, and p16^{INK4a} viruses were plated on poly-D-lysine–coated chambers and cultured in the presence (+) and absence (−) of FGF2 and EGF. The percentage of pyknotic dead cells was quantified at DAP0 and DAP2. (E) Stimulation of NSC self-renewal by transient activation of Myc. (left) A schematic diagram of experimental conditions. MycER is a fusion construct between human c-Myc and the hormone-binding domain of the estrogen receptor α and is conditionally and reversibly activated by 4-hydroxytamoxifen (4-OHT; Eilers, M., D. Picard, K.R. Yamamoto, and J.M. Bishop. 1989. *Nature*. 340:66–68). Neurospheres derived from E13.5 rat forebrains were infected with control and MycER viruses and grown with (+) and without (−) 1 μM 4-OHT for 48 h. After removal of 4-OHT, the cells were subjected to the serial clonal neurosphere formation assays. (right) The frequency of neurosphere-forming cells after first and second passages of E13.5 neurospheres infected with control and MycER viruses treated with and without 4-OHT. *, $P < 0.01$; **, $P < 0.05$ compared with control virus–infected cells (without 4-OHT in E). Error bars indicate mean + SD.

Genotype of E11.5 mouse embryos from *c-Myc*$^{+/-}$;*p19*$^{ARF+/-}$, *c-Myc*$^{+/-}$;*p19*$^{ARF-/-}$, and *c-Myc*$^{+/-}$;*p53*$^{+/-}$ matings

	c-Myc$^{+/-}$;*p19*$^{ARF+/-}$ x *c-Myc*$^{+/-}$;*p19*$^{ARF+/-}$	*c-Myc*$^{+/-}$;*p19*$^{ARF-/-}$ x *c-Myc*$^{+/-}$;*p19*$^{ARF-/-}$	*c-Myc*$^{+/-}$;*p53*$^{+/-}$ x *c-Myc*$^{+/-}$;*p53*$^{+/-}$
Number of breeding pairs	4	7	4

Genotype						
c-Myc	*p19*^{ARF}			*c-Myc*	*p53*	
+/+	+/+	0	–	+/+	+/+	5
+/+	+/–	7	–	+/+	+/–	2
+/+	–/–	2	13	+/+	–/–	3
+/–	+/+	3	–	+/–	+/+	4
+/–	+/–	8	–	+/–	+/–	10
+/–	–/–	5	32	+/–	–/–	3
–/–	+/+	0 (3)	–	–/–	+/+	0 (2)
–/–	+/–	0 (5)	–	–/–	+/–	0 (5)
–/–	–/–	0 (1)	0 (10)	–/–	–/–	0 (1)
Total number of embryos		25	45			27

Figure S4. **Failure of rescue of the early lethality of *c-Myc*$^{-/-}$ mutation by inactivation of *p19*^{ARF} and *p53*.** *c-Myc*$^{-/-}$ mutants die before E10.5 (Davis, A.C., M. Wims, G.D. Spotts, S.R. Hann, and A. Bradley. 1993. *Genes Dev.* 7:671–682). Thus, the genotypes of embryos obtained by crossing heterozygous *c-Myc* mutants with *p19*^{ARF} and *p53* heterozygous or homozygous mutants were analyzed at E11.5. The number of breeding pairs and embryos with the indicated genotypes are summarized. The numbers in parentheses indicate embryos that were partially absorbed or abnormally small.

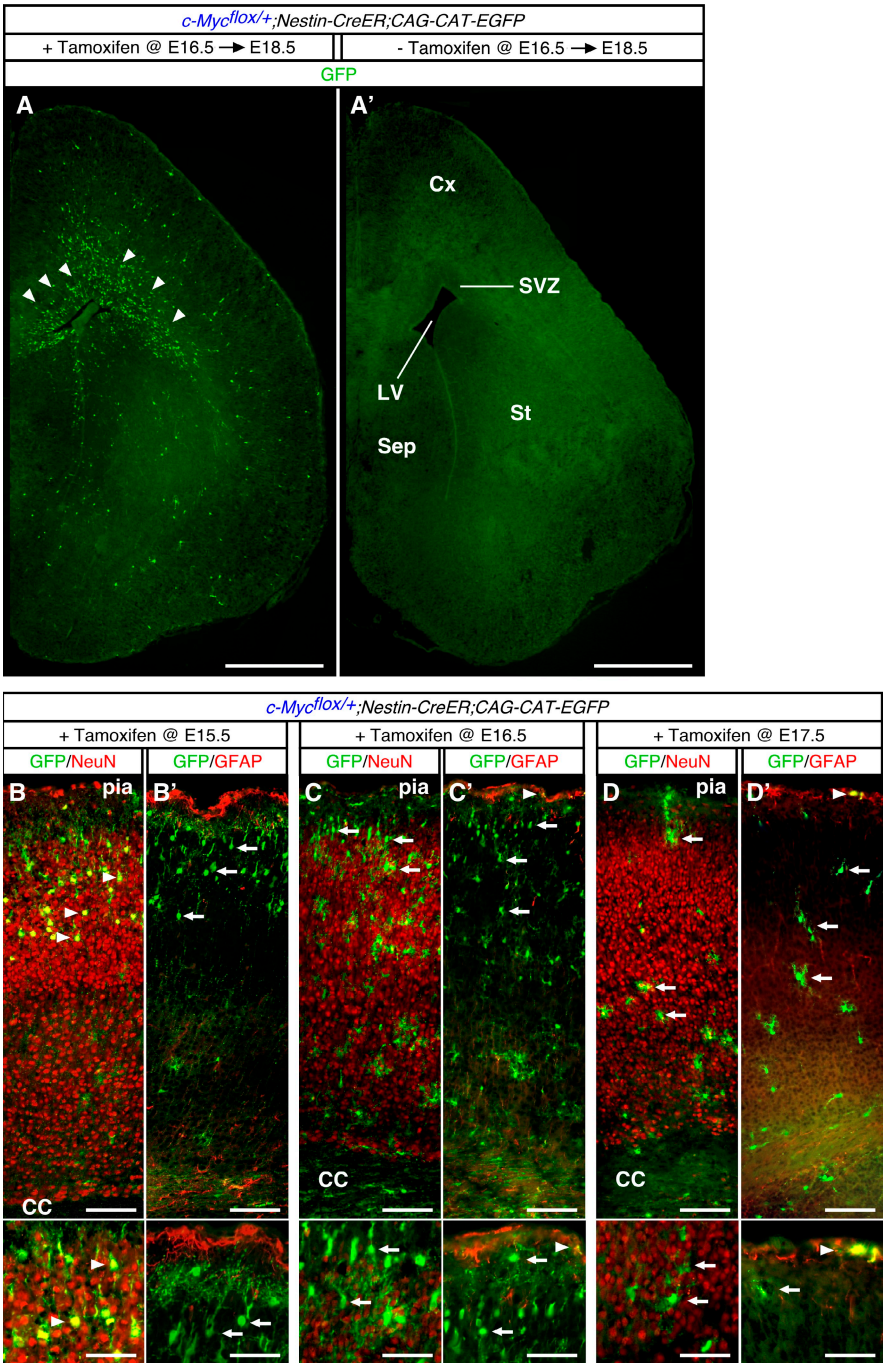

Figure S5. **Stage-dependent genetic labeling of neural progenitors using *Nestin-CreER;CAG-CAT-EGFP* mice.** (A and A′) Tamoxifen-dependent labeling of neural progenitors in vivo. *c-Myc*$^{flox/+}$*;Nestin-CreER;CAG-CAT-EGFP* mice were treated with (left, +) and without (right, −) tamoxifen at E16.5 and analyzed at E18.5. 2 d after tamoxifen treatment, the vast majority of GFP-labeled cells were detected in or around the subventricular zone (SVZ) lining the lateral ventricles (A, arrowheads). These late-stage progenitors in the subventricular zone have been shown to be Olig2$^+$ glial progenitors that disperse the brain parenchyma and differentiate into astrocytes and oligodendrocytes at the postnatal stage (Marshall, C.A., S.O. Suzuki, and J.E. Goldman. 2003. *Glia*. 43:52–61; Marshall, C.A., B.G. Novitch, and J.E. Goldman. 2005. *J. Neurosci*. 25:7289–7298). In contrast, no GFP$^+$ cells were detected in untreated animals (A′), indicating the tamoxifen dependency of recombination of the floxed *GFP* allele. (B–D′) Tamoxifen was administered to pregnant dams at E15.5 (B and B′), 16.5 (C and C′), and 17.5 (D and D′), and brains were analyzed at P2–5. Coronal sections of the dorsolateral neocortex of control *c-Myc*$^{flox/+}$*;Nestin-CreER;CAG-CAT-EGFP* mice were double stained for GFP and the mature neuronal marker NeuN (B–D) or the astrocyte marker GFAP (B′–D′). Top panels show the whole thickness of the neocortex (the pial surface on the top), and bottom panels show higher magnification views of the areas near the pial surface. When tamoxifen was administered at E15.5, the stage before gliogenesis begins, the vast majority of GFP$^+$ recombined cells became NeuN$^+$ neurons (B, arrowheads), whereas few GFP$^+$ cells were GFAP$^+$ (B′, arrows) postnatally. Consistent with their late-stage generation, these GFP$^+$/NeuN$^+$ neurons occupied the top layers of the neocortex. (C and D) In contrast, when recombination was induced at E16.5 and E17.5, a much smaller fraction of recombined cells were destined to become neurons (7–9% and 0.5–1.0%, respectively). (C–D′, arrows) Instead, many GFP$^+$ cells scattered along the whole depth of the neocortex as well as the underlying subcortical white matter and corpus callosum (CC). In *c-Myc*$^{flox/+}$*;Nestin-CreER;CAG-CAT-EGFP* mice, a small fraction of GFP$^+$ cells localized beneath the pial surface began to express GFAP at P2 and P3 (C′ and D′, arrowheads). The expression of GFAP in these cells becomes prominent at later postnatal stages (Burns, K.A, A.E. Ayoub, J.J. Breunig, F. Adhami, W.L. Weng, M.C. Colbert, P. Rakic, and C.Y. Kuan. 2007. *Cereb Cortex*. 17:2585–2592). Cx, neocortex; LV, lateral ventricle; Sep, septum; St, striatum. Bars: (A and A′) 500 µm; (B–D′, top) 100 µm; (B–D′, bottom) 50 µm.